Brain & Development 41 (2019) 829–838

BRAIN & DEVELOPMENT
Official Journal of the Japanese Society of Child Neurology

www.elsevier.com/locate/braindev

Original article

Activation of leukocyte immunoglobulin-like receptor B2 signaling pathway in cortical lesions of pediatric patients with focal cortical dysplasia type IIb and tuberous sclerosis complex

Jiong Yue, Chunqing Zhang, Xianjun Shi, Yujia Wei, Lihong Liu, Shiyong Liu, Hui Yang *

Epilepsy Research Center of PLA, Department of Neurosurgery, Xinqiao Hospital, Army Medical University (Third Military Medical University), Chongqing, China

Received 19 April 2019; received in revised form 24 July 2019; accepted 13 August 2019

Abstract

Backgrounds: Focal cortical dysplasia type IIb (FCD IIb) and tuberous sclerosis complex (TSC) are very frequently associated with epilepsy in pediatric patients. Human leukocyte immunoglobulin-like receptor B2 (LILRB2) participates in the process of neurite growth, synaptic plasticity, and inflammatory reaction, suggesting a potential role of LILRB2 in epilepsy. However, little is known about the distribution and expression of LILRB2 in cortical lesions of FCD IIb and cortical tubers of TSC.

Methods: In this study, we have described the distribution and expression of LILRB2 signaling pathway in cortical lesions of pediatric patients with FCD IIb (n = 15) and TSC (n = 12) relative to age-matched autopsy control samples (CTX, n = 10), respectively. The protein levels of LILRB2 pathway molecules were assessed by western blotting and immunohistochemistry. The expression pattern was investigated by immunohistochemistry and double labeling experiment. Spearman correlation analysis to explore the correlation between LILRB2 protein level and seizure frequency.

Results: The protein levels of LILRB2 and its downstream molecules POSH, SHROOM3, ROCK1, ROCK2 were increased in cortices of patients compared to CTX. Protein levels of LILRB2 negatively correlated with the frequency of seizures in FCD IIb and TSC patients, respectively. Moreover, all LILRB2 pathway molecules were strongly expressed in dysmorphic neurons, balloon cells, and giant cells, LILRB2 co-localized with neuron marker and astrocyte marker.

Conclusion: Taken together, the special expression patterns of LILRB2 signaling pathway in cortical lesions of FCD IIb and TSC implies that it may be involved in the process of epilepsy.

Keywords: Focal cortical dysplasia; Tuberous sclerosis complex; Malformations of cortical development; LILRB2; PirB; Inflammation

1. Introduction

Two important subtypes of malformations of cortical development (MCDs), focal cortical dysplasia type IIb (FCD IIb) and tuberous sclerosis complex (TSC) are common causes of medically refractory epilepsy, particularly in children [1]. It is believed that FCD IIb and TSC are due to architectural and/or cellular

* Corresponding author at: Epilepsy Research Center of PLA, Department of Neurosurgery, Xinqiao Hospital, Army Medical University, 183 Xinqiao Main Street, Shapingba District, Chongqing 400037, China.
E-mail address: huiyangxq@163.com (H. Yang).

https://doi.org/10.1016/j.braindev.2019.08.002
0387-7604/

abnormalities that mainly occur during critical period in the development of the brain. An increasing body of evidence suggests that FCD IIb and TSC share a common genetic background, especially somatic pathogenic variants in genes of PI3K/AKT/mTOR pathway [2]. It is noteworthy that genetic abnormalities in TSC are mainly manifested in the mutation of TSC1 or TSC2 genes. Multiple authors have brought new insight into and provided solid evidence for the involvement of TSC1 and TSC2 in FCD IIb [2,3]. On the other hand, histopathologically, the lesions of FCD IIb and TSC both showed cortical disorganized lamination, with dysmorphic neurons and balloon cells or giant cells. Therefore, the present study investigated the FCD IIb and TSC-related epilepsy.

Human leukocyte immunoglobulin-like receptor B2 (LILRB2), as the murine paired immunoglobulin-like receptor B (PirB) homolog, was originally identified in the cells of the immunologic system, including myelomonocytic cells and lymphoid cells, playing an immunosuppressive function [4,5]. Accumulated evidence confirms that LILRB2 and PirB are also expressed in neurons and astrocytes in various regions of the central nervous system (including the hippocampus, cerebral cortex, spinal cord and cerebellum, etc.) under normal or pathophysiological conditions [6,7]. LILRB2 and PirB act as receptors for major histocompatibility complex class I (MHCI) and myelin associated inhibitors (MAIs), mainly restricting neurite growth and synaptic remodeling [8–10]. Notably, further experiments confirmed that the scaffold proteins of SH3s (POSH), actin-myosin regulatory protein SHROOM3, and Rho Kinase (ROCK1/2) are key downstream molecules of LILRB2 (PirB) pathway to transfer inhibition function [11,12]. Starkey et al. revealed that PirB located on neuronal axons and dendrites plays an important role in age-related hippocampal aging, such as changes in synaptic homeostasis and neurotransmitter release [13]. Mice lacking PirB display stronger long-term potentiation (LTP), fainter long-term depression (LTD), and higher-frequency miniature excitatory postsynaptic current (mEPSC) on L2/3 and L5 pyramidal neurons, moreover the number of excitatory synapses and dendritic spine density are also elevated [14,15]. LILRB2 is strongly expressed in human Alzheimer's disease (AD) brains and acts as a receptor for β-amyloid, which can impair synaptic plasticity and cause synaptic loss [16]. Thus, LILRB2 (PirB) pathway is involved in regulating neurite elongation, synaptic stability and synaptic plasticity. We have previously provided data on the expression characteristics of LILRB2 (PirB) pathway in temporal lobe epilepsy (TLE) patients and animal models. We found that LILRB2 signaling pathway is mainly activated in neurons and astrocytes in the TLE lesions compared with normal temporal cortex tissue taken from surgical excision of traumatic brain injury patients [6]. In this study, we aimed to define the expression and cellular distribution of LILRB2 signaling pathway in FCD IIb and TSC pediatric epileptic patients.

2. Materials and methods

2.1. Subjects and clinical data

This study and all its procedures were approved by the ethics committee of the Army Medical University, China. And the human brain specimens were used in a manner compliant with the Declaration of Helsinki. This study obtained informed consent from the guardians of all individuals.

A total of 27 specimens from medically intractable epilepsy patients with FCD IIb ($n = 15$) and TSC ($n = 12$) were examined in the present study. Diagnosis of FCD IIb and TSC are according to the criteria established by the International League Against Epilepsy (ILAE). Clinical mutation analyses of the TSC1 and TSC2 loci were performed by denaturing high-performance liquid chromatography (DHPLC) to confirm our diagnoses. The clinical characteristics derived from the patient's medical records are summarized in (Table 1). The histologically normal cortex tissues were obtained at autopsy from 10 control patients without a history of seizures or other neurological diseases. All the autopsies were performed within 6 h after death. Within this post-mortem interval, it is well documented that most proteins are stable and therefore well preserved [17]. Two neuropathologists also helped to review the autopsy cases, and both gross and microscopic examinations revealed no structural abnormality. Relevant clinical data for controls are summarized in (Table 2).

2.2. Tissue preparation

Tissues were immediately divided into two parts at the time of surgery or autopsy. One was immediately frozen in liquid nitrogen and stored at −80 °C for western blotting analysis. The other samples were fixed in 4% phosphate-buffered formalin for 48 h, and tissues were then embedded in paraffin, sectioned at 6 μm thickness for immunohistochemistry and 10 μm for double immunofluorescence staining.

2.3. Western blotting

Total proteins were extracted from tissues using the whole protein extraction kit (Beyotime Institute of Biotechnology, Jiangsu, China). The total tissue lysates were centrifuged at 12,000 g for 15 min at 4 °C, and the protein concentration in the supernatant was determined using the bicinchoninic acid (BCA) protein assay (Bio-Rad, Hercules, CA, USA). Equal amounts of protein (60 μg/lane) were separated by sodium dodecyl

Table 1
Clinical and neuropathological features of patients with FCD IIb and TSC.

Case no.	Gender	Diagnosis	TSC genotype	Age (year)	Duration (year)	AEDs	Seizure frequency per month	Epileptic foci	PO
1	M	FCD IIb	NMI	2.2	0.8	VPA, CBZ, PB	48	F	I
2	M	FCD IIb	TSC1	4.0	1.7	OXC, VPA, PHT	22	O	II
3	F	FCD IIb	TSC2	1.7	0.3	CBZ, VPA, ACTH	13	T	I
4	M	FCD IIb	NMI	4.1	2.5	CBZ, VPA	114	F	I
5	F	FCD IIb	NMI	5.9	3.0	VPA, LEV	94	P, O	III
6	F	FCD IIb	NMI	8.0	5.5	OXC, VPA, LEV	82	T	III
7	M	FCD IIb	NMI	11	6.3	OXC, VPA, GBP	19	F	I
8	F	FCD IIb	NMI	2.5	1.0	CBZ, VPA	76	P	II
9	M	FCD IIb	NMI	5.3	2.0	CBZ, VPA, TPM	100	F, T	II
10	F	FCD IIb	TSC1	4.8	3.2	VPA, CBZ, PHT	88	O	I
11	M	FCD IIb	TSC1	12.5	4.0	OXC, VPA	11	T	I
12	M	FCD IIb	TSC2	3.5	2.9	VPA, LEV, ACTH	103	F	III
13	F	FCD IIb	NMI	6.4	1.5	CBZ, VPA, TPM	68	F	II
14	F	FCD IIb	NMI	2.4	0.8	OXC, VPA, PHT	49	T	I
15	M	FCD IIb	NMI	5.0	3.0	CBZ, PHT, VPA, ACTH	116	T	II
16	F	TSC	TSC2	8.9	5.5	OXC, PHT	11	O	I
17	F	TSC	NMI	7.5	5.4	OXC, VPA	58	F	II
18	M	TSC	TSC1	4.0	2.2	CBZ, PHT, TMP	77	T	II
19	F	TSC	TSC2	3.0	1.6	CBZ, PHT, LTG	15	T	I
20	M	TSC	TSC1	10	4.0	CBZ, PHT	35	F	III
21	M	TSC	TSC1	4.5	3.3	CBZ, VPA, ACTH	22	O	II
22	M	TSC	TSC2	8.0	4.5	VPA, LEV	32	P, O	I
23	F	TSC	TSC2	7.0	0.6	CBZ, LTG	20	T	II
24	F	TSC	TSC1	2.0	1.5	CBZ, VPA, ACTH	29	F	II
25	M	TSC	TSC1	3.7	1.9	OXC, CBL, VPA	118	T	III
26	F	TSC	TSC2	3.9	2.0	OXC, VPA	58	F, O	III
27	F	TSC	NMI	11	5.0	OXC, VPA, ACTH	68	F	I

F, female. M, male. NMI, no mutation identified by genetic analysis. AED, antiepileptic drugs. CBZ, carbamazepine. VPA, valproic acid. CLB, clonazepam. GBP, gabapentin. LTG, lamotrigine. OXC, oxcarbazepine. PB, phenobarbital. PHT, phenytoin. TPM, topiramate. ACTH, adrenocorticotropic hormone. F, frontal lobe. T, temporal lobe. P, parietal lobe. O, occipital lobe. PO, postoperative outcome (Engel class).

Table 2
Clinical data from 10 autopsy control samples.

Case no.	Gender	Age (year)	Cause of death	Neuropathology	PMI (h)	Seizure
1	M	2.6	Electric shock	Normal	4.0	None
2	M	4.8	renal failure	Normal	1.8	None
3	M	2.3	Motor vehicle accident	Normal	5.5	None
4	F	6.1	Motor vehicle accident	Normal	4.5	None
5	F	9.0	Drowning	Normal	3.1	None
6	M	3.7	Motor vehicle accident	Normal	2.5	None
7	F	3.3	Electric shock	Normal	1.2	None
8	F	11.2	Drowning	Normal	4.7	None
9	M	9.0	Motor vehicle accident	Normal	3.2	None
10	F	2.0	renal failure	Normal	2.9	None

F, female. M, male. PMI, postmortem interval, that is, interval between death of a patient and removal of the brain before freezing or fixation.

sulfate–polyacrylamide gel electrophoresis (SDS-PAGE) (5% spacer gel, 80 V, 25 min; 10% separating gel, 120 V, 60 min) and electrophoretically transferred to polyvinylidene fluoride (PVDF) membranes (Millipore, Temecula, CA, USA) using a semi-dry electroblotting system (Transblot SD; Bio-Rad) (80 min, 300 mA). Next, membranes were incubated at room temperature for 2 h in 5% not-fat dry milk to block nonspecific binding. Then the membranes were incubated overnight at 4 °C with relevant primary antibodies: anti-LILRB2 (mouse monoclonal, 1:500; R & D Systems, Minneapolis, MN); anti-POSH (rabbit polyclonal, 1:300; Biosynthesis Biotechnology, Beijing, China); anti-SHROOM3 (goat polyclonal, 1:500; T-17; Santa Cruz Biotechnology, Santa Cruz, CA, USA); anti-ROCK1 (rabbit polyclonal, 1:500; Proteintech, China); anti-ROCK2 (rabbit polyclonal, 1:500; Proteintech, China) and anti-GAPDH (rabbit polyclonal, 1:10000; Abcam, Cambridge, United Kingdom). After several washes in TBST (20 mmol/l Tris-HCl, pH 8.0, 150 mmol/l NaCl, 0.5% Tween-20), the samples were treated with horseradish peroxidase-conjugated goat anti-rabbit, goat anti-mouse, or rabbit anti-goat secondary antibody (1/1000; Zhongshan Golden bridge Biotechnology, China) for 1 h in a 37 °C incubator. The immunoreactive bands were visualized using enhanced chemiluminescence and were scanned and analyzed with Quantity One software (Bio-Rad Laboratories, Hercules, CA, USA).

2.4. Immunohistochemistry and double-labeled immunofluorescence

Paraffin sections were deparaffinized in xylene and rehydrated through a graduated alcohol series. Endogenous peroxidase activity was blocked with 3% H2O2 in methyl alcohol. All of the samples were placed into phosphate buffered saline (0.01 M, pH 7.3) and heated 20 min in a microwave oven for antigen retrieval. Sections were then blocked in bovine serum (Boster Biological Technology, Wuhan, China) with 1% Triton X-100 (Sigma, St Louis, MO) for 60 min at room temperature. After removal of excess serum, sections were incubated with primary antibody overnight at 4 °C. The following primary antibodies were used: anti-LILRB2 (mouse monoclonal, 1:100; R & D Systems, Minneapolis, MN); anti-POSH (rabbit polyclonal, 1:100; Biosynthesis Biotechnology, Beijing, China); anti-SHROOM3 (goat polyclonal, 1:100; T-17; Santa Cruz Biotechnology, Santa Cruz, CA, USA); anti-ROCK1 (rabbit polyclonal, 1:500; Proteintech, China); anti-ROCK2 (rabbit polyclonal, 1:500; Proteintech, China). Then, the sections were incubated with goat anti-rabbit, goat anti-mouse, or rabbit anti-goat immunoglobulin conjugated to peroxidase-labeled dextran polymer (EnVision + System-HRP; Boster, China) for 1 h at 37 °C, and subsequently incubated in 3,3-diaminobenzidine (DAB, Boster) for the appropriate time. The sections were counterstained with hematoxylin, dehydrated, and coverslipped. No immunoreactive cells were observed in negative control experiments, which included omission of the primary antibody, pre-absorption with a tenfold excess of specific blocking antigen, or incubation with an isotype-matched rabbit polyclonal antibody.

For double immunofluorescence staining, anti-LILRB2 (mouse monoclonal, 1:100; R & D Systems, Minneapolis, MN) combined with anti-NF200 (rabbit monoclonal, 1:100; Abcam, Britain), anti-GFAP (rabbit monoclonal, 1:100; Boster), and anti-Iba1 (rabbit polyclonal, 1:100; Biosynthesis Biotechnology, Beijing, China) overnight at 4 °C, respectively. Then the sections were incubated with a mixture of Alexa Fluor 594 antibodies and FITC-conjugated antibodies (1:300, Invitrogen) for 1 h at 37 °C. Next, 4′,6-diamidino-2-phenylindole (DAPI, 10 μg/ml, Beyotime, China) was used to counterstain the cell nuclei. The fluorescent signals were acquired using a confocal fluorescence microscope (TCS-TIV; Leica, Nussloch, Germany).

2.5. Evaluation of immunostaining

The evaluation of specific immunoreactivity, and the presence or absence of various histopathological parameters were assessed by two independent observers blind

to clinical data. Relevant methods can be referred to previous studies [18,19]. The overall concordance was greater than 90%, and the overall κ value ranged from 0.83 to 0.95. When a disagreement occurred, independent reevaluation was performed by both observers to define he final score. Using a Leica microscope to examine a total microscopic area of 781.250 μm^2 (200 high-power nonoverlapping fields of 0.0625×0.0625 mm width, using a square grid inserted into the eyepiece) in each section. The intensity of staining was evaluated using a semi-quantitative three-point scale where IR was defined as the following: absent (−, 0), weak (+, 1), moderate (+ +, 2), or strong (+ + +, 3) (Table 3). These scores represent the predominant staining intensity in each section and were calculated as the average of the selected fields.

2.6. Statistical analysis

The SPSS Statistical 16 package (SPSS Inc., IL, Chicago, USA) was used for statistical analyses. Data were expressed as mean ± standard deviation (S.D.). One-way analysis of variance (ANOVA) analysis was used to determine the differences. The correlations between variables were evaluated by the Spearman rank correlation test. Following the statistical tests, $p < 0.05$ were considered statistically significant.

3. Results

3.1. Comparison of clinical variables

5 female and 5 male individuals in control group with a mean age of 5.400 ± 3.278 years (range, 2.0 to 11.2 years). The mean age of the FCD IIb and TSC pediatric epileptic patients was 5.659 ± 3.043 years (range, 1.7–12.5 years), with 13 males and 14 females. An examination of gender and age indicated no difference between the autopsy controls and epileptic groups (FCD IIb and TSC) ($P > 0.05$).

3.2. Western blotting and immunohistochemistry analysis of LILRB2

We used western blotting to examine the protein levels of LILRB2 in total homogenates from normal control cortex (n = 10), FCD IIb lesions (n = 15), and TSC tubers specimens (n = 12). The LILRB2 protein expression were upregulated in both the FCD IIb and TSC lesions compared with control tissues ($P < 0.05$; Fig. 1A–B). Furthermore, the correlation analysis showed that the LILRB2 protein concentration in patients with FCD IIb and TSC was negatively correlated with preoperative seizure frequency (Fig. 1C–D).

In controls, weak LILRB2 immunoreactivity in neurons and glial cells were observed in gray matter and white matter, respectively (Fig. 2A–B). Moderate to strong LILRB2 immunostaining in the dysmorphic neurons, balloon cells, and glial cells were detected in the FCD IIb specimens (Fig. 2C–D). Giant cells, dysmorphic neurons, glial cells in TSC tubers expressed LILRB2 with considerable intensity (Fig. 2E–F). The immunoreactivity scores of LILRB2 in epileptic groups (FCD IIb and TSC) were dramatically higher than those in the controls ($P < 0.001$) (Table 3). Double-labeled immunofluorescence experiments demonstrated that LILRB2 was colocalized with NF200 in dysmorphic neurons (Fig. 2G, J) and giant cells (Fig. 2J), and the astrocyte marker GFAP (Fig. 2H, K), but not with Iba1 in microglia (Fig. 2I, L).

3.3. POSH, SHROOM, ROCK1, and ROCK2 expression

Increased POSH ($P < 0.05$), SHROOM3 ($P < 0.01$), ROCK1 ($P < 0.05$), and ROCK2 ($P < 0.05$) protein expression levels in FCD IIb and TSC specimens compared with controls were confirmed by Western blotting. Representative immunoblots and densitometric quantification are shown in Fig. 3.

With immunohistochemistry analysis, faint or intermediate POSH, SHROOM, ROCK1, and ROCK2 immunostaining in neurons and glial cells (Fig. 4A–D). Moderate to strong immunostaining in dysmorphic neurons, balloon cells, and glial cells in FCD IIb specimens (Fig. 4E–H). In TSC, moderate and strong POSH, SHROOM3, ROCK1, and ROCK2 immunostaining were observed in dysmorphic neurons, giant cells, and glial cells (Fig. 4I–L). The immunoreactivity scores of POSH, SHROOM3, ROCK1, and ROCK2 in epileptic groups were higher compared with the control samples ($P < 0.001$) (Table 3).

Table 3
Immunoreactivity scores.

	Control (n = 10)	FCD IIb (n = 15)	TSC (n = 12)
LILRB2	1.10 ± 0.71	1.98 ± 0.73#	1.93 ± 0.65#
POSH	1.27 ± 0.59	2.37 ± 0.76#	2.06 ± 0.77#
SHROOM3	1.38 ± 0.56	2.04 ± 0.75#	2.13 ± 0.54#
ROCK1	1.24 ± 0.70	2.10 ± 0.70#	1.95 ± 0.61#
ROCK2	1.08 ± 0.64	2.16 ± 0.67#	2.12 ± 0.73#

The data are expressed as the means ± SD, FCD IIb or TSC vs. control specimens. One-way analysis of variance. #$P < 0.001$.

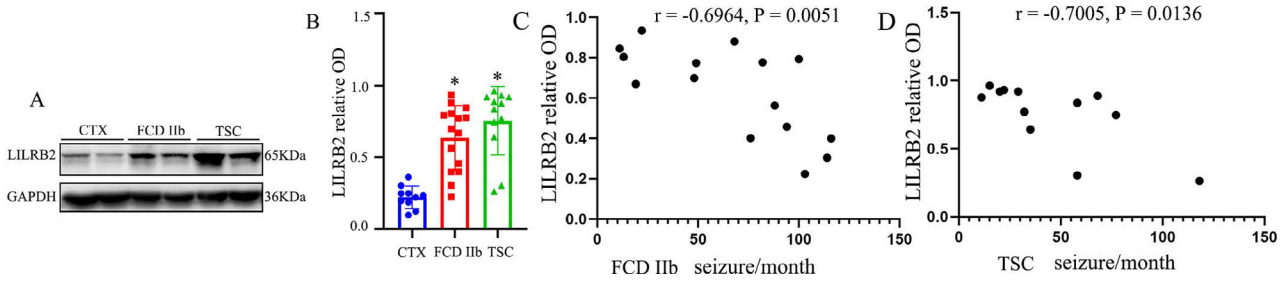

Fig. 1. The expression of LILRB2 in total homogenates from normal control cortex (CTX), FCD IIb lesions, and TSC tubers specimens. Representative immunoblot (A) and densitometric quantification (B) showing immunoreactive protein levels for LILRB2 were significantly increased in FCD IIb and TSC compared with CTX subjects. (C, D) Scatter plot showing the significant negative correlation between the protein levels (relative optical density [OD]) of LILRB2 and seizure frequency (seizures per month), Spearman rank correlation coefficient: $r = -0.6964$, $P = 0.0051$ for FCD IIb. $r = -0.7005$, $P = 0.0136$ for TSC ($n = 10$ for controls, $n = 15$ for FCD IIb patients, $n = 12$ for TSC patients). The data are expressed as the means ± SD. *$P < 0.05$.

4. Discussion

In this study, we used western blotting, immunohistochemistry and fluorescence labeling to explore the expression patterns of LILRB2 signaling pathway molecules, found that LILRB2 signaling pathway proteins were up-regulated in FCD IIb and TSC lesions compared with autopsy control samples, and mainly over-expressed in dysmorphic neurons, balloon cells, giant cells, and glial cells. Intriguingly, the protein levels of LILRB2 in FCD IIb and TSC lesions negatively correlated with the frequency of seizures. Moreover, LILRB2 co-localized with neuron marker (NF200) and astrocyte marker (GFAP), but not with microglia marker (Iba1). Based on these data, we suggest that LILRB2 signaling pathway may be involved in the pathophysiology or epileptogenesis of human FCD IIb and TSC.

Overall, epilepsy is a complex network disease. Many studies have indicated that the cortical lesions of FCD IIb and cortical tubers of TSC are intrinsic epileptogenic zones and are highly associated with epilepsy. Moreover, large and poorly-differentiated cells with neuronal and glial characteristics, such as balloon cells of FCD IIb and giant cells of TSC, are often the unique features of these types of MCDs and are closely related to the epileptogenicity [20,21]. Abnormal excitatory network connections in epileptogenic lesions may be one of the main causes of recurrent epileptic seizures. Growing evidence indicates that LILRB2 (PirB) signaling pathway is regulated by MHCI and myelin inhibitors (NogoA, MAG, OMgp) to inhibit neurite regeneration and prolongation [8–10]. Notably, previous research has verified that NogoA and MHCI were upregulated in resected epileptic lesions of FCD, TSC, and TLE patients [22–24]. On the other hand, in visual cortex of mice lacking PirB, the density of functional glutamatergic synapses is more than 50% higher than wildtype [14]. mEPSC frequency in hippocampal CA1 pyramidal cells is increased in PirB gene deletion mice, consistent with a greater density of excitatory synapses and altered synapse pruning [25]. Further mechanism study revealed that PirB regulates synaptic plasticity through N-methyl-D-aspartate receptor (NMDAR), which a key excitatory glutamatergic receptor for epileptiform activity transmission [25]. In the present study, we found that LILRB2 signaling pathway was over-activated in cortical lesions of FCD IIb and TSC, and relevant factors LILRB2, POSH, SHROOM3, ROCK1, and ROCK2 are primarily over-expressed in membrane, cytoplasm and neurites of misshapen cells. Hence, it can be inferred that elevated LILRB2 pathway factors in misshapen cells of FCD IIb and TSC cortical lesions may adjust the formation of abnormal excitatory neural circuits cored by misshapen cells, and regulate the function of excitatory transmission. Of course, it may be more convincing and fascinating to observe the structure and/ or function of excitatory circuits in MCD epileptic models with PirB gene overexpression or in clinical fresh MCD lesion slices treated with human LILRB2 purified protein.

Inflammatory processes, especially activation of astrocytes, and release of inflammatory mediators, contribute to epileptogenesis, and the development of spontaneous seizure activity. Astrocyte proliferation and the production of related inflammatory cytokines have been confirmed to be involved in the pathophysiological process of MCD-related epilepsy [26,27]. Inhibitory LILRB2 and PirB, negatively regulates immune and inflammation responses, and is crucial to dendritic cell maturation, B cell suppression, and to balancing Th1 and Th2 immune responses [28]. For instance, the loss of PirB in macrophages aggravated the inflammatory response and increased the release of IL-6, IL-1β and TNF-α under the stimulation of bacteria [29,30]. Our study confirmed that LILRB2 was overexpressed in GFAP-positive reactive astrocytes in FCD IIb and TSC lesions. On this basis, we speculate that LILRB2 activation in astrocytes may play an important role in the inflammatory response and the release of inflammatory cytokines in FCD IIb and TSC lesions. Noticeably, whether it plays a protective role by inhibiting the

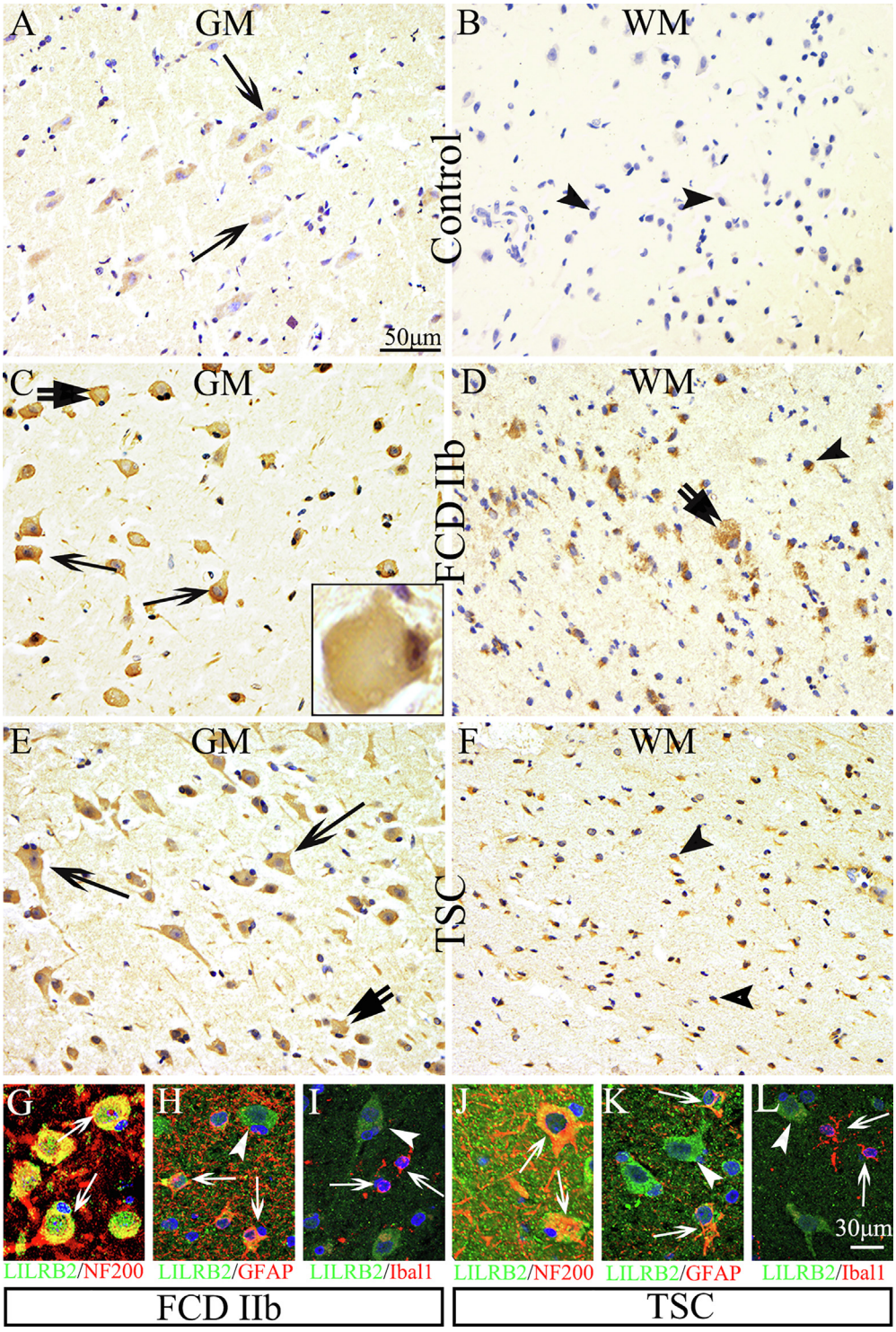

Fig. 2. Histopathologic features of LILRB2 in control, the lesions of FCD IIb and tubers of TSC. (A, B) weak LILRB2 immunoreactivity in neurons (gray matter, GM, arrows in A) and glial cells (white matter, WM, arrowheads in B) of controls. (C, D) Moderate to strong LILRB2 immunoreactivity in dysmorphic neurons (arrows), balloon cells (double arrows and insert of C), glial cells (arrowheads) in FCD IIb GM and WM lesions. (E, F) Very obvious LILRB2 staining of giant cells (double arrows in GM), dysmorphic neurons (arrows in GM), glial cells (arrowheads in WM) in tubers. (G–I) Double labeling in cortical lesions of FCD IIb specimens. Co-localization of LILRB2 (green) with NF200 (red) in dysmorphic neurons (yellow, arrows in G). LILRB2 (green) and GFAP (red) were also co-localized in astrocytes (arrows in H, arrowhead: dysmorphic neuron). LILRB2 (green) not co-expressed with Iba1 (red, arrows in I, arrowhead: dysmorphic neuron). (J–L) Double labeling in tubers of TSC. LILRB2 co-expressed with NF200 in dysmorphic neurons and giant cells (yellow, arrows in J). LILRB2 co-labeled with GFAP (arrows in K, arrowheads: dysmorphic neuron), not Iba1 (red, arrows in L, arrowhead: dysmorphic neuron). (n = 10 for controls, n = 15 for FCD IIb patients, n = 12 for TSC patients) .Scale bars: A–F, 50 μm. G–L, 30 μm. (For interpretation of the references to colour in this figure legend, the reader is referred to the web version of this article.)

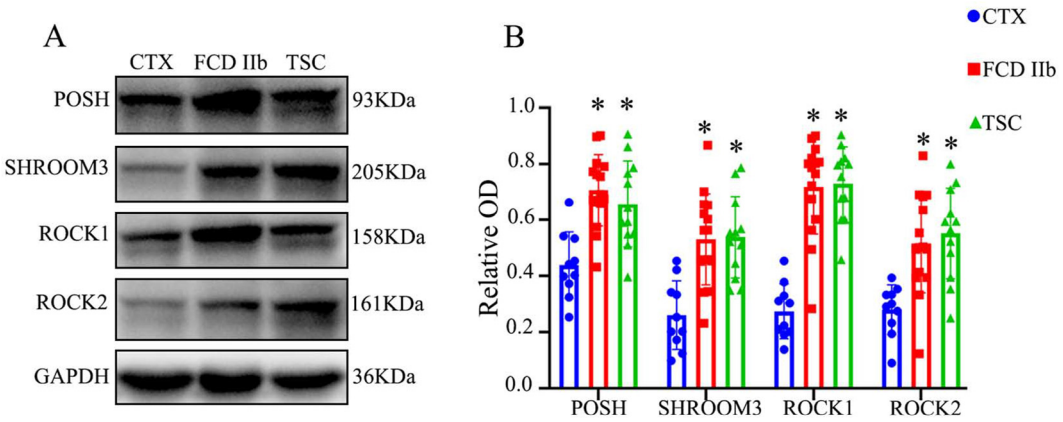

Fig. 3. Protein expression of POSH, SHROOM, ROCK1, and ROCK2 in CTX, FCD IIb and TSC. (A) Representative immunoblot of POSH (93 kDa), SHROOM3 (205 kDa), ROCK1 (158 kDa), ROCK2 (161 kDa) in total homogenates from CTX, the lesions of FCD IIb and tubers of TSC. The expression of internal control protein GAPDH (36 kDa) was shown in the same protein extracts. (B) Densitometric quantification show that protein levels of POSH, ROCK1, and ROCK2 are elevated in FCD IIb and TSC compared with CTX, respectively. (n = 10 for controls, n = 15 for FCD IIb patients, n = 12 for TSC patients). The data are expressed as the means ± SD. *P < 0.05.

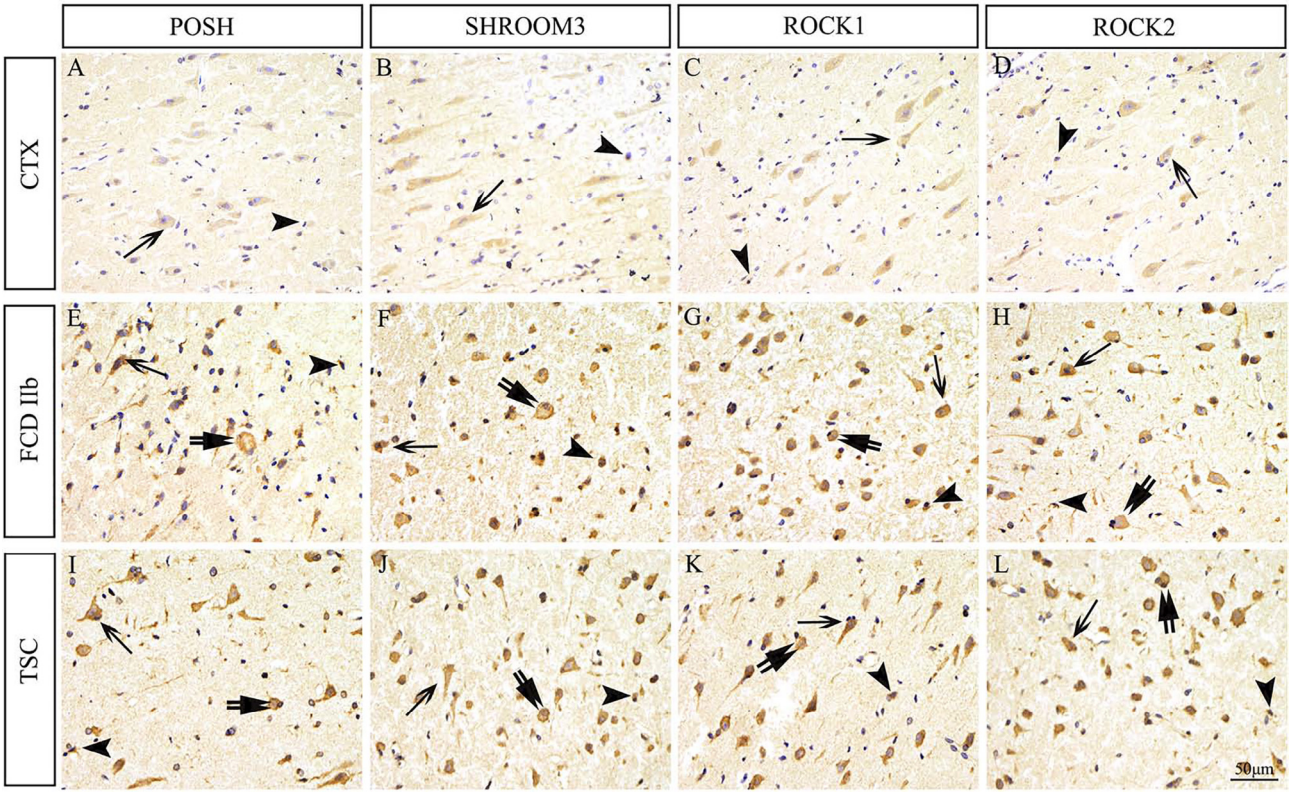

Fig. 4. Immunostaining for POSH, SHROOM, ROCK1, and ROCK2 in CTX, the lesions of FCD IIb and tubers of TSC. (A–D) In CTX group, Faint POSH, SHROOM, ROCK1 and ROCK2 immunoreactivity in neurons (arrows), and in glial cells (arrowheads). (E–H) In FCD IIb group, moderate to strong immunostaining in dysmorphic neurons (arrows), balloon cells (double arrows), and in glial cells (arrowheads). (I–L) Enhanced immunostaining in dysmorphic neurons (arrows), giant cells (double arrows), and glial cells (arrowheads) in TSC. (n = 10 for controls, n = 15 for FCD IIb patients, n = 12 for TSC patients). Scale bar: 50 μm for all panels.

initiation and deterioration of inflammation in epileptogenic zone may require further investigation.

Interestingly, the expression of LILRB2 in epileptogenic foci of FCD IIb and TSC was negatively correlated with the frequency of seizures, which was consistent with our previous analysis of the relationship between LILRB2 and TLE. This seems to suggest that LILRB2 may inhibit epileptic seizures. Certainly, it

should not be excluded that the frequency and severity of epileptic seizures may also affect the expression of LILRB2 in epileptogenic lesions.

Hemimegalencephaly (HME) is a rare malformation of cortical development (associated with developmental delay and severe epilepsy), characterized by enlargement of an entire cerebral hemisphere. HME share some pathological features and somatic mutant genes with FCD IIb [31]. Unfortunately, HME was not included in this study since we did not get enough cases during our study period.

In conclusion, this is the first time to explore the expression patterns of LILRB2 signaling pathway molecules in surgically resected epileptic foci of FCD IIb and TSC. Our immunohistochemistry, immunofluorescence, and western blotting demonstrated LILRB2 signaling pathway is over-activated on the misshapen cells (dysmorphic neurons, balloon cells, and giant cells) and astrocytes. Following the current descriptive study, further investigation is needed to elucidate whether LILRB2 can inhibit the formation and/ or function of excitatory circuits and the inflammatory response process during epileptogenesis of FCD IIb and TSC.

Acknowledgements

We sincerely thank all the patients and their families for their participation. This work was supported by National Natural Science Foundation of China (NO.81771217, NO.81771394).

Appendix A. Supplementary data

Supplementary data to this article can be found online at https://doi.org/10.1016/j.braindev.2019.08.002.

References

[1] Barkovich AJ, Dobyns WB, Guerrini R. Malformations of cortical development and epilepsy. Cold Spring Harb Perspect Med 2015;5 a022392.
[2] Benova B, Jacques TS. Genotype-phenotype correlations in focal malformations of cortical development: a pathway to integrated pathological diagnosis in epilepsy surgery. Brain Pathol 2018.
[3] Lim JS, Gopalappa R, Kim SH, Ramakrishna S, Lee M, Kim WI, et al. Somatic mutations in TSC1 and TSC2 cause focal cortical dysplasia. Am J Hum Genet 2017;100:454–72.
[4] Mori Y, Tsuji S, Inui M, Sakamoto Y, Endo S, Ito Y, et al. Inhibitory immunoglobulin-like receptors LILRB and PIR-B negatively regulate osteoclast development. J Immunol 2008;181:4742–51.
[5] Hirayasu K, Arase H. Functional and genetic diversity of leukocyte immunoglobulin-like receptor and implication for disease associations. J Hum Genet 2015;60:703–8.
[6] Yue J, Li W, Liang C, Chen B, Chen X, Wang L, et al. Activation of LILRB2 signal pathway in temporal lobe epilepsy patients and in a pilocarpine induced epilepsy model. Exp Neurol 2016;285:51–60.
[7] Nakamura Y, Fujita Y, Ueno M, Takai T, Yamashita T. Paired immunoglobulin-like receptor B knockout does not enhance axonal regeneration or locomotor recovery after spinal cord injury. J Biol Chem 2011;286:1876–83.
[8] Filbin MT. PirB, a second receptor for the myelin inhibitors of axonal regeneration Nogo66, MAG, and OMgp: implications for regeneration in vivo. Neuron 2008;60:740–2.
[9] Adelson JD, Barreto GE, Xu L, Kim T, Brott BK, Ouyang YB, et al. Neuroprotection from stroke in the absence of MHCI or PirB. Neuron 2012;73:1100–7.
[10] Syken J, Grandpre T, Kanold PO, Shatz CJ. PirB restricts ocular-dominance plasticity in visual cortex. Science 2006;313:1795–800.
[11] Dickson HM, Zurawski J, Zhang H, Turner DL, Vojtek AB. POSH is an intracellular signal transducer for the axon outgrowth inhibitor Nogo66. J Neurosci 2010;30:13319–25.
[12] Taylor J, Chung KH, Figueroa C, Zurawski J, Dickson HM, Brace EJ, et al. The scaffold protein POSH regulates axon outgrowth. Mol Biol Cell 2008;19:5181–92.
[13] VanGuilder Starkey HD, Van Kirk CA, Bixler GV, Imperio CG, Kale VP, Serfass JM, et al. Neuroglial expression of the MHCI pathway and PirB receptor is upregulated in the hippocampus with advanced aging. J Mol Neurosci 2012;48:111–26.
[14] Djurisic M, Vidal GS, Mann M, Aharon A, Kim T, Ferrao Santos A, et al. PirB regulates a structural substrate for cortical plasticity. Proc Natl Acad Sci U S A 2013;110:20771–6.
[15] Bochner DN, Sapp RW, Adelson JD, Zhang S, Lee H, Djurisic M, et al. Blocking PirB up-regulates spines and functional synapses to unlock visual cortical plasticity and facilitate recovery from amblyopia. Sci Transl Med 2014;6:258ra140.
[16] Kim T, Vidal GS, Djurisic M, William CM, Birnbaum ME, Garcia KC, et al. Human LilrB2 is a β-amyloid receptor and its murine homolog PirB regulates synaptic plasticity in an Alzheimer's model. Science 2013;341:1399–404.
[17] Hynd MR, Lewohl JM, Scott HL, Dodd PR. Biochemical and molecular studies using human autopsy brain tissue. J Neurochem 2003;85:543–62.
[18] Toering ST, Boer K, de Groot M, Troost D, Heimans JJ, Spliet WG, et al. Expression patterns of synaptic vesicle protein 2A in focal cortical dysplasia and TSC-cortical tubers. Epilepsia 2009;50:1409–18.
[19] Zhang CQ, Shu HF, Yin Q, An N, Xu SL, Yin JB, et al. Expression and cellular distribution of vascular endothelial growth factor-C system in cortical tubers of the tuberous sclerosis complex. Brain Pathol 2012;22:205–18.
[20] Wong M. Mechanisms of epileptogenesis in tuberous sclerosis complex and related malformations of cortical development with abnormal glioneuronal proliferation. Epilepsia 2008;49:8–21.
[21] Blümcke I, Thom M, Aronica E, Armstrong DD, Vinters HV, Palmini A, et al. The clinicopathologic spectrum of focal cortical dysplasias: a consensus classification proposed by an ad hoc Task Force of the ILAE Diagnostic Methods Commission1. Epilepsia 2011;52:158–74.
[22] Prabowo AS, Iyer AM, Anink JJ, Spliet WG, van Rijen PC, Aronica E. Differential expression of major histocompatibility complex class I in developmental glioneuronal lesions. J Neuroinflammation 2013;10:12.
[23] Bandtlow CE, Dlaska M, Pirker S, Czech T, Baumgartner C, Sperk G. Increased expression of Nogo-A in hippocampal neurons of patients with temporal lobe epilepsy. Eur J Neurosci 2004;20:195–206.
[24] Yu SX, Li S, Shu HF, Zhang CQ, Liu SY, Yang H. Expression of the Nogo-A system in cortical lesions of pediatric patients with tuberous sclerosis complex and focal cortical dysplasia type IIb. J Neuropathol Exp Neurol 2012;71:665–77.

[25] Djurisic M, Brott BK, Saw NL, Shamloo M, Shatz CJ. Activity-dependent modulation of hippocampal synaptic plasticity via PirB and endocannabinoids. Mol Psychiatry 2018.
[26] Zurolo E, Iyer A, Maroso M, Carbonell C, Anink JJ, Ravizza T, et al. Activation of Toll-like receptor, RAGE and HMGB1 signalling in malformations of cortical development. Brain 2011;134:1015–32.
[27] Boer K, Jansen F, Nellist M, Redeker S, van den Ouweland AM, Spliet WG, et al. Inflammatory processes in cortical tubers and subependymal giant cell tumors of tuberous sclerosis complex. Epilepsy Res 2008;78:7–21.
[28] Takeda K, Nakamura A. Regulation of immune and neural function via leukocyte Ig-like receptors. J Biochem 2017;162:73–80.
[29] Nakayama M, Underhill DM, Petersen TW, Li B, Kitamura T, Takai T, et al. Paired Ig-like receptors bind to bacteria and shape TLR-mediated cytokine production. J Immunol 2007;178:4250–9.
[30] Munitz A, Cole ET, Beichler A, Groschwitz K, Ahrens R, Steinbrecher K, et al. Paired immunoglobulin-like receptor B (PIR-B) negatively regulates macrophage activation in experimental colitis. Gastroenterology 2010;139:530–41.
[31] D'Gama AM, Geng Y, Couto JA, Martin B, Boyle EA, LaCoursiere CM, et al. Mammalian target of rapamycin pathway mutations cause hemimegalencephaly and focal cortical dysplasia. Ann Neurol 2015;77:720–5.